

Sec. 9.3.3 Fermi Gas and Density of States

Classical description: Momentum $p = mv$ Kinetic Energy $E = mv^2/2 = p^2/2m$

Quantum description: $p_x = \hbar k_x$

All conduction electrons are equally spread out in the k space (reciprocal space)

Available space in k

Table A.1. Properties of coordinate and k space in one, two, and three dimensions

Coordinate Region	k -Space Unit Cell	Fermi Region	Value of k^2	Dimensions
Length L	$2\pi/L$	$2k_F$	k_X^2	One
Area $A = L^2$	$(2\pi/L)^2$	πk_F^2	$k_X^2 + k_Y^2$	Two
Volume $V = L^3$	$(2\pi/L)^3$	$4\pi k_F^3/3$	$k_X^2 + k_Y^2 + k_Z^2$	Three

Table A.2. Number of electrons $N(E)$ and density of states $D(E) = dN(E)/dE$ as function of energy E for electrons delocalized in one, two, and three spatial dimensions, where $A = L^2$ and $V = L^3$

Number of Electrons N	Density of States $D(E)$	Delocalization Dimensions
$N(E) = \frac{4k_F}{2\pi/L} = \frac{2L}{\pi} \left(\frac{2m}{\hbar^2}\right)^{1/2} E^{1/2}$	$\frac{dN(E)}{dE} D(E) = \frac{L}{\pi} \left(\frac{2m}{\hbar^2}\right)^{1/2} E^{-1/2}$	1
$N(E) = \frac{2\pi k_F^2}{(2\pi/L)^2} = \frac{A}{2\pi} \left(\frac{2m}{\hbar^2}\right) E$	$D(E) = \frac{A}{2\pi} \left(\frac{2m}{\hbar^2}\right)$	2
$N(E) = \frac{2(4\pi k_F^3/3)}{(2\pi/L)^3} = \frac{V}{3\pi^2} \left(\frac{2m}{\hbar^2}\right)^{3/2} E^{3/2}$	$D(E) = \frac{V}{2\pi^2} \left(\frac{2m}{\hbar^2}\right)^{3/2} E^{1/2}$	3

Single Electron Tunneling

Capacitance of a dielectric disk : $C = 8\epsilon_0\epsilon_r r$

Capacitance of a dielectric sphere : $C = 4\epsilon_0\epsilon_r r$

For a GaAs sphere, $C = 1.47 \times 10^{-18} r$ farad for radius r in nm

VOLUME 63, NUMBER 7 p. 801 PHYSICAL REVIEW LETTERS

14 AUGUST 1989

Scanning-Tunneling-Microscope Observations of Coulomb Blockade and Oxide Polarization in Small Metal Droplets

R. Wilkins,⁽¹⁾ E. Ben-Jacob,^(1,2) and R. C. Jaklevic⁽³⁾

⁽¹⁾Department of Physics, The University of Michigan, Ann Arbor, Michigan 48109

⁽²⁾School of Physics and Astronomy, Raymond and Beverly Sackler Faculty of Exact Sciences,

Tel Aviv University, 69978 Tel Aviv, Israel

⁽³⁾Scientific Laboratory, Ford Motor Company, Dearborn, Michigan 48121

(Received 20 March 1989)

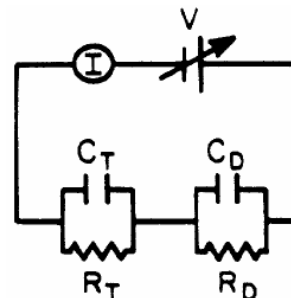
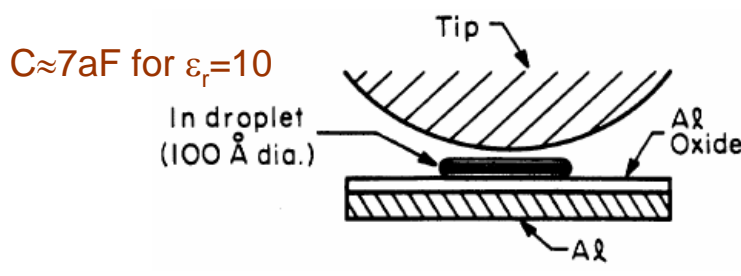


FIG. 1. Schematic showing an In droplet separated from an Al ground plane by a tunneling oxide layer ($\approx 10 \text{ \AA}$ thickness) with an Au STM tip positioned about 10 \AA above it. The equivalent circuit is shown with a voltage source and capacitor C_T for tip to droplet and C_D for droplet to ground plane. The resistors characterize the tunneling probability for each junction and are strictly shot-noise devices.

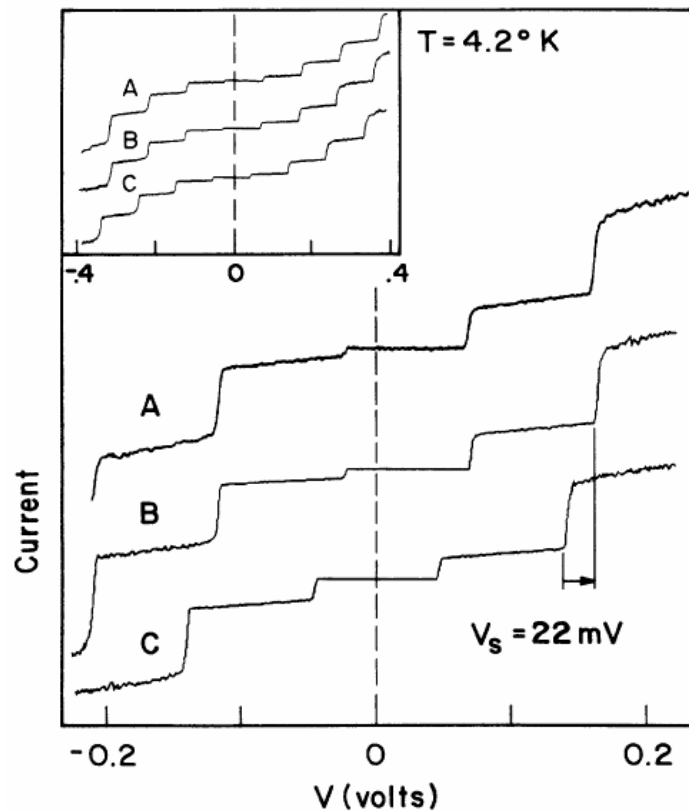
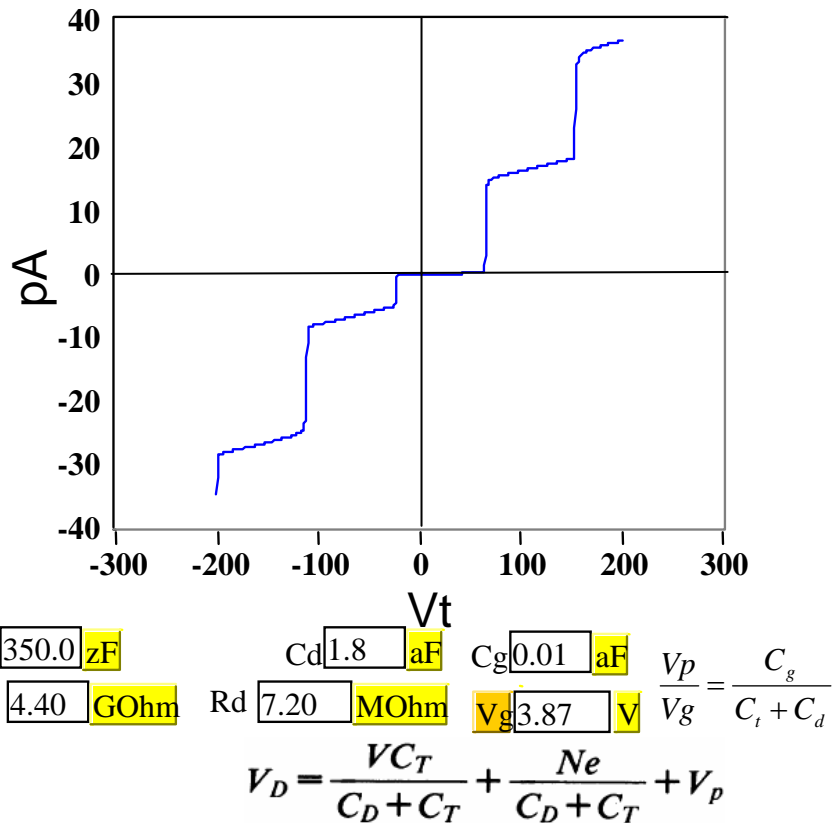


FIG. 2. Curve *A* is an experimental *I*-*V* characteristic from an In droplet in a sample with average droplet size of 300 Å. The peak-peak current is 1.8 nA. Curve *B* is a theoretical fit to the data for $C_D = 3.5 \times 10^{-19}$ F, $C_T = 1.8 \times 10^{-18}$ F, $R_D = 7.2 \times 10^6$ Ω, and $R_T = 4.4 \times 10^9$ Ω. The obvious asymmetric features in curve *A* require a voltage shift $V_s = 22$ mV ($V_p = 18$ mV). Curve *C*, calculated for $V_s = 0$, shows the (seldom observed) symmetric case. As explained in the text, a small quadratic term was added to the computed tunneling rate for each junction. Inset: A wider voltage scan for this same droplet; again, the topmost curve is experimental data.



by scanning the substrate.¹⁴ However, we do not understand at this time why C_T is greater than C_D . At $T = 4$

Nano-particles:

1. Contains many electrons:

- normal metal nano-particles
- superconductor nano-particles
- magnetic nano-particles

2. Contains few electrons

Subjects:

1. Device structures:

- for particles: nano-pore, electrodes with small gap
- for 2DEG devices: lateral and pillar types

2. Physics:

in many electron system:

Level statistics

Parity effect

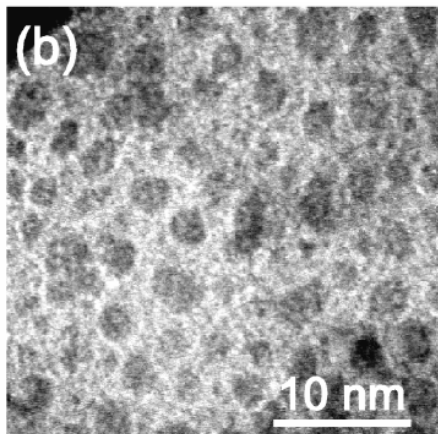
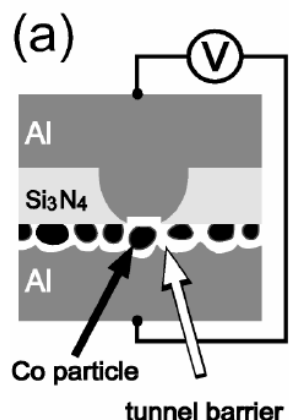
Lande g factor (spin-orbit interaction)

superconductivity

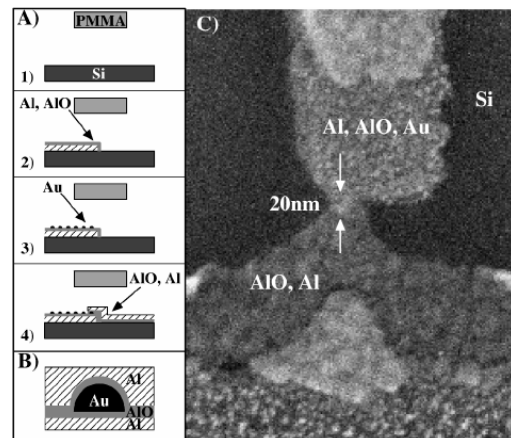
Magnetic moment

in few electron system:

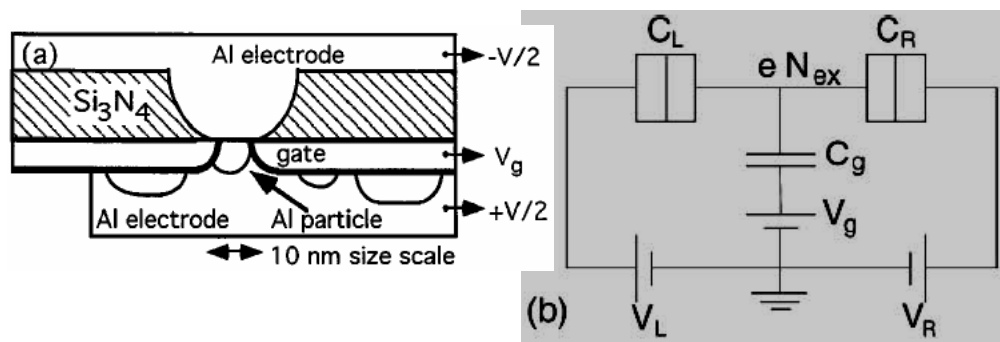
Shell filling; artificial atom



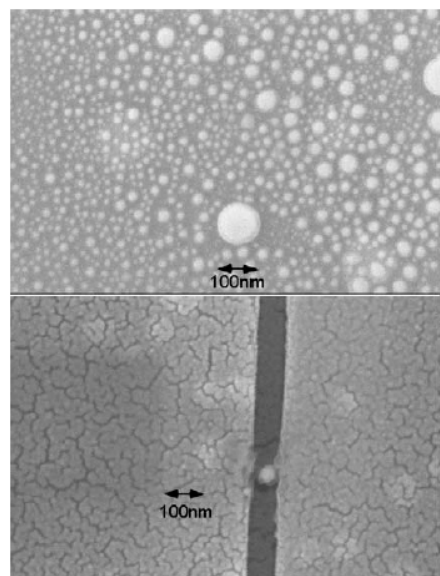
Tunneling via Individual Electronic States in Ferromagnetic Nanoparticles
PRL, 83, 4148 (99)



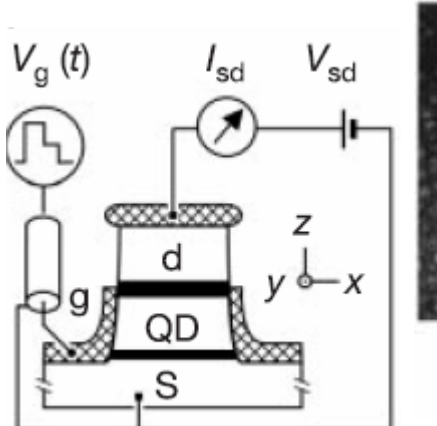
Spectroscopy, Interactions, and Level Splittings in Au Nanoparticles
PRL, 83, 1644 (99)



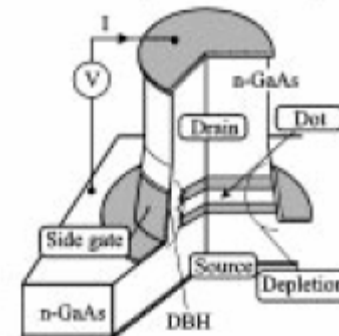
Gate-Voltage Studies of Discrete Electronic States in Aluminum Nanoparticles
PRL, 78, 4087 (97)



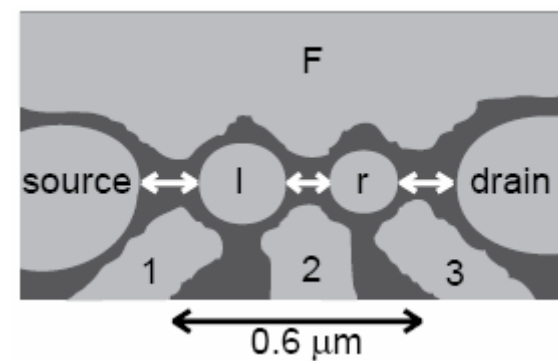
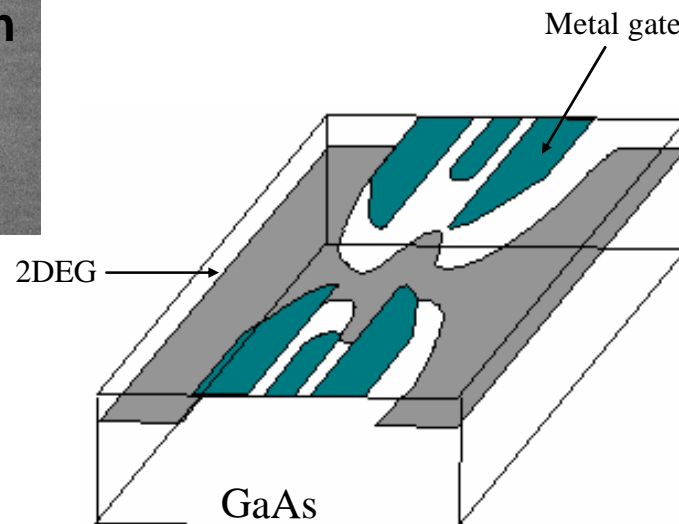
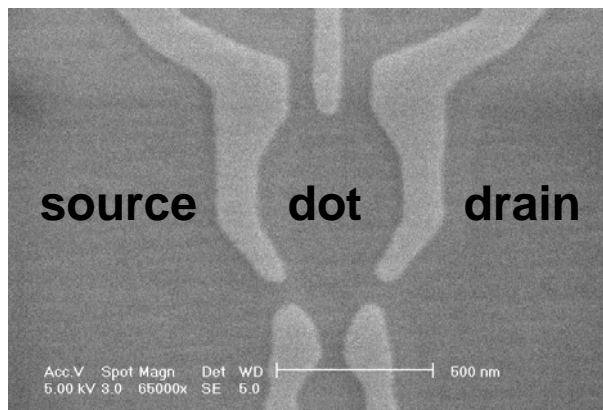
Electron transport in Metallic grains
(short note by D. Davidovic et al.)



Allowed and forbidden transitions in artificial hydrogen and helium atoms
Nature 419, 278 (02)



Shell Filling and Spin Effects in a Few Electron Quantum Dot
PRL, 77, 3613 (96)



Microwave spectroscopy of a quantum-dot molecule
Nature, 395, 873 (98)

Relevant energy scales (1)

Charging energy:

$$E_C = e^2 / 2C_{\Sigma} \quad C_{\Sigma} = C_{Sj} + C_{Dj} + C_g$$

$$C_{Sj} \approx 0.045 \text{ aF/nm}^2 \times A_{\text{junction}} \quad 100 \text{ nm}^2 \rightarrow 8 \text{ meV} = 93 \text{ K}$$

For an embedded nano particle: $E_C \approx 0.8 \text{ eV nm}^2 / r^2$

Mean level spacing:

$$\delta = \frac{2}{D(\varepsilon_F)} = \frac{2}{\frac{Vol}{2\pi^2} \left(\frac{2m}{\hbar^2} \right)^{3/2} E^{1/2}} = \frac{2\pi^2 \hbar^2}{mk_F Vol} = \frac{1.50 \text{ eV nm}^2}{k_F Vol} = \frac{2.86 \text{ eV nm}^2}{k_F \text{ diameter}^3}$$

$D(\varepsilon_F)$ = density of states at Fermi level

$$\text{Number of electrons } N(\varepsilon_F) = \frac{Vol}{3\pi^2} \left(\frac{2m}{\hbar^2} \right)^{3/2} E^{3/2} = \frac{Vol}{3\pi^2} k_F^3 = 0.0177 k_F^3 \text{ diameter}^3$$

$r = 5 \text{ nm, Al particle: } k_F = 17.5 \text{ nm}^{-1}, \delta = 1.3 \text{ meV}, N = 11858$

$r = 5 \text{ nm, Au particle: } k_F = 12.1 \text{ nm}^{-1}, \delta = 1.9 \text{ meV}, N = 3920$

Relevant energy scales (2)

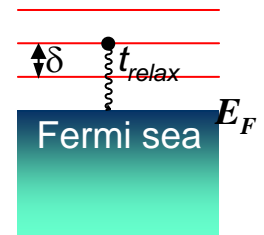
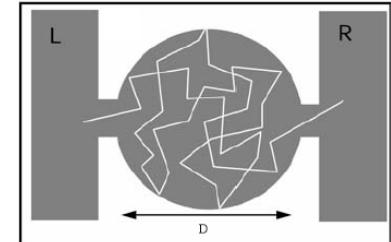
Thouless energy $\approx \begin{cases} \frac{\hbar D_{diff}}{r^2} = \frac{\hbar v_F l}{3r^2} = \frac{0.25k_F l}{r^2} \text{ meV nm}^2 & (\text{diffusive}) \\ \frac{\hbar v_F (3r/2a^*)}{r^2} = \frac{\hbar v_F}{2ar} = \frac{38k_F}{ar} \text{ meV nm}^2 & (\text{ballistic}) \end{cases}$

Delft and Ralph, Phys. Rep. 345, 61 (01), Eq. 5

$\delta > E_{\text{Thouless}}$: well resolvable discrete levels

Small Thouless energy usually implies a longer relaxation time

$$\delta \geq \hbar/t_{\text{relax}} \quad \text{for well resolvable discrete levels}$$



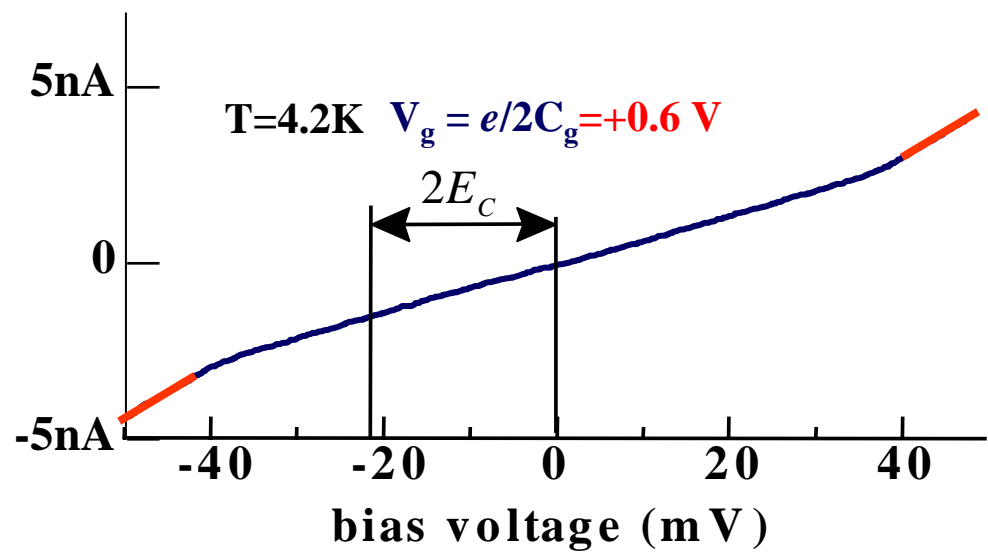
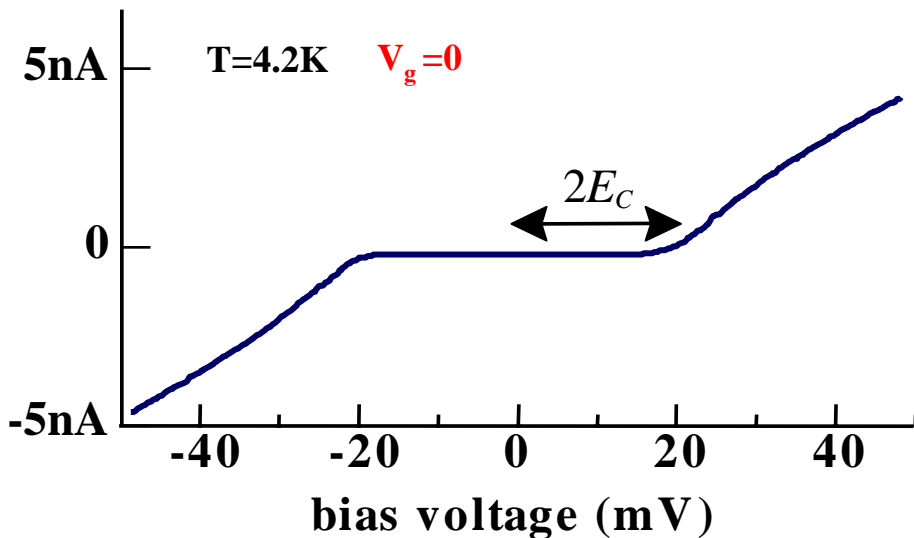
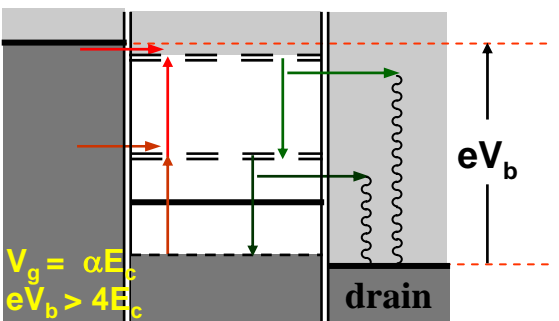
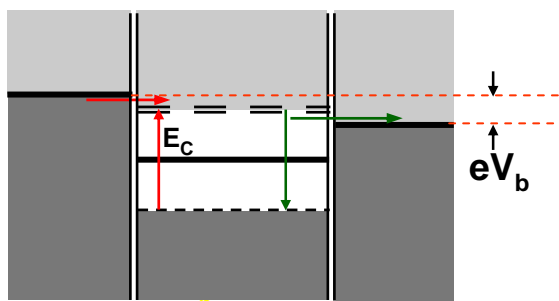
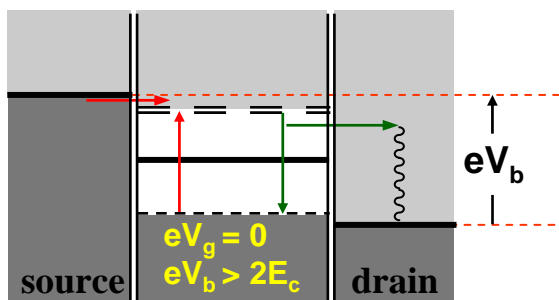
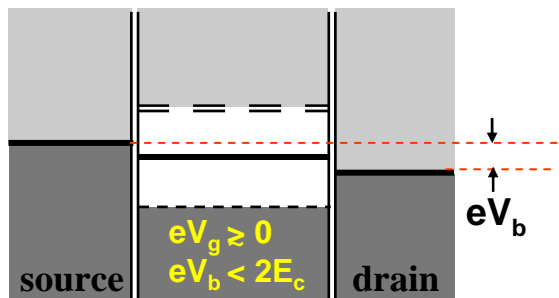
Tunneling time: t_{tunnel} $\delta \geq \hbar/t_{\text{tunnel}}$ for well resolvable discrete levels

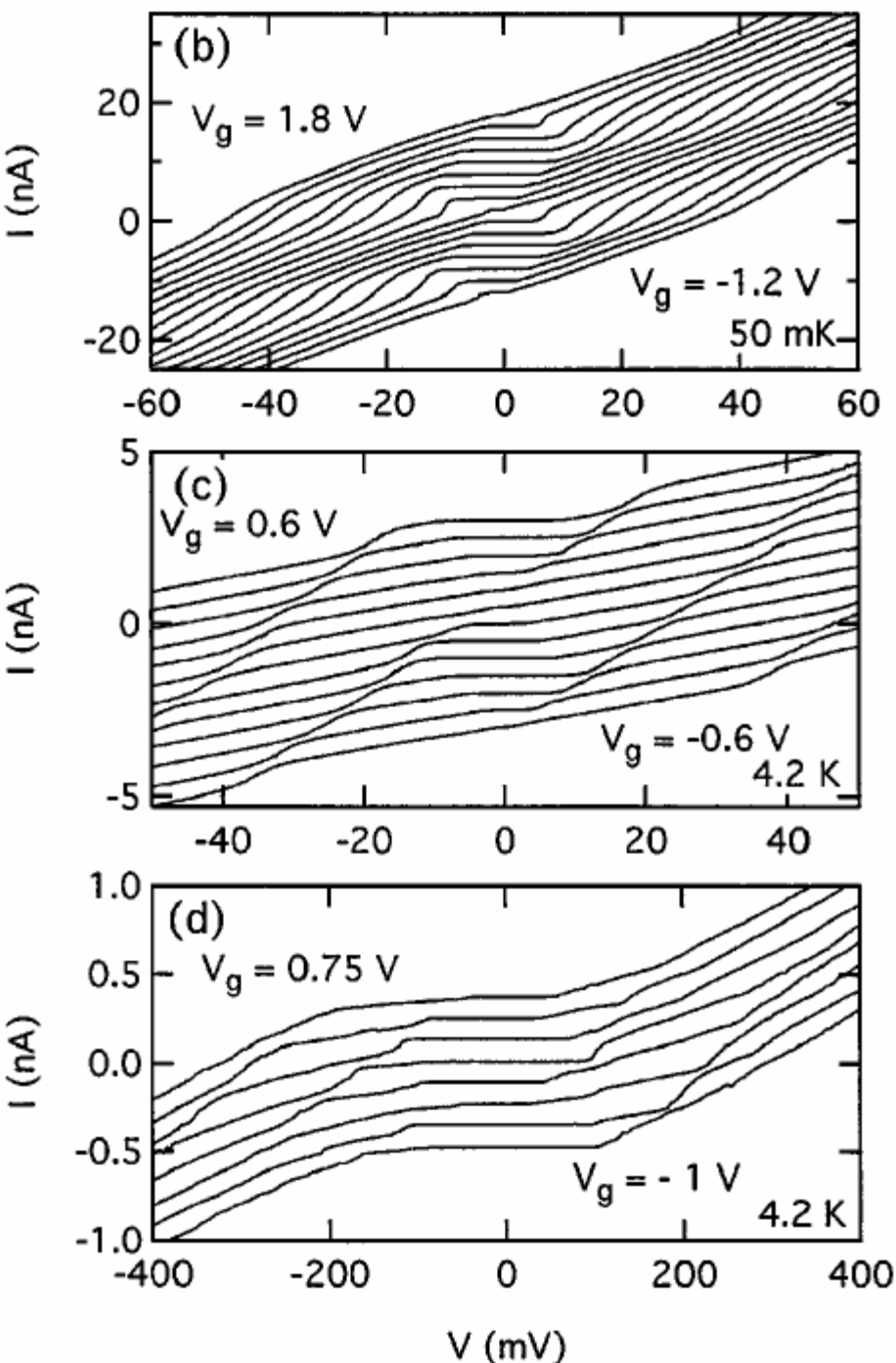
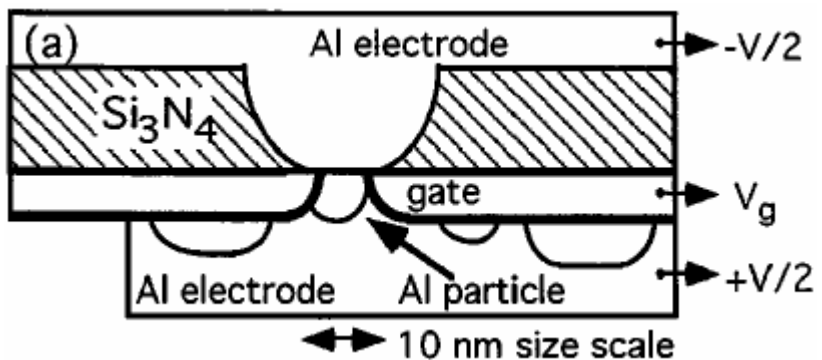
The same argument applies for Coulomb blockade:

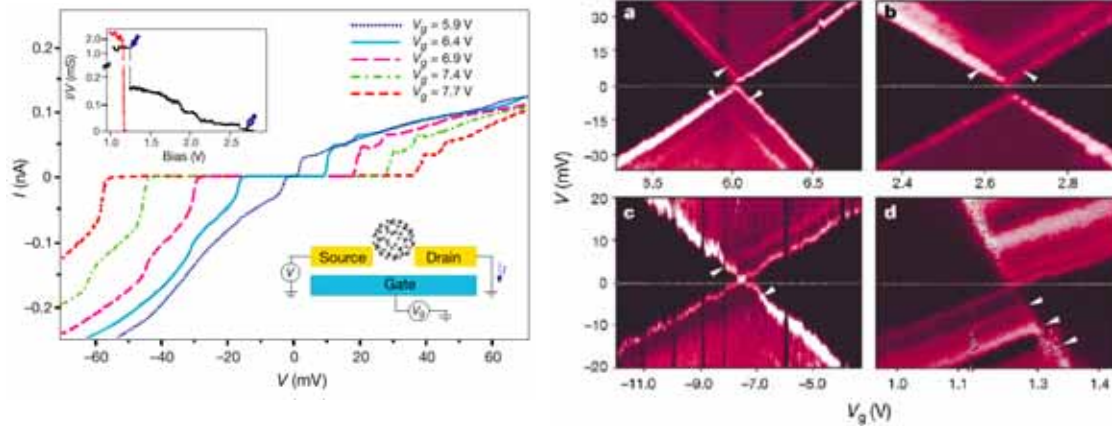
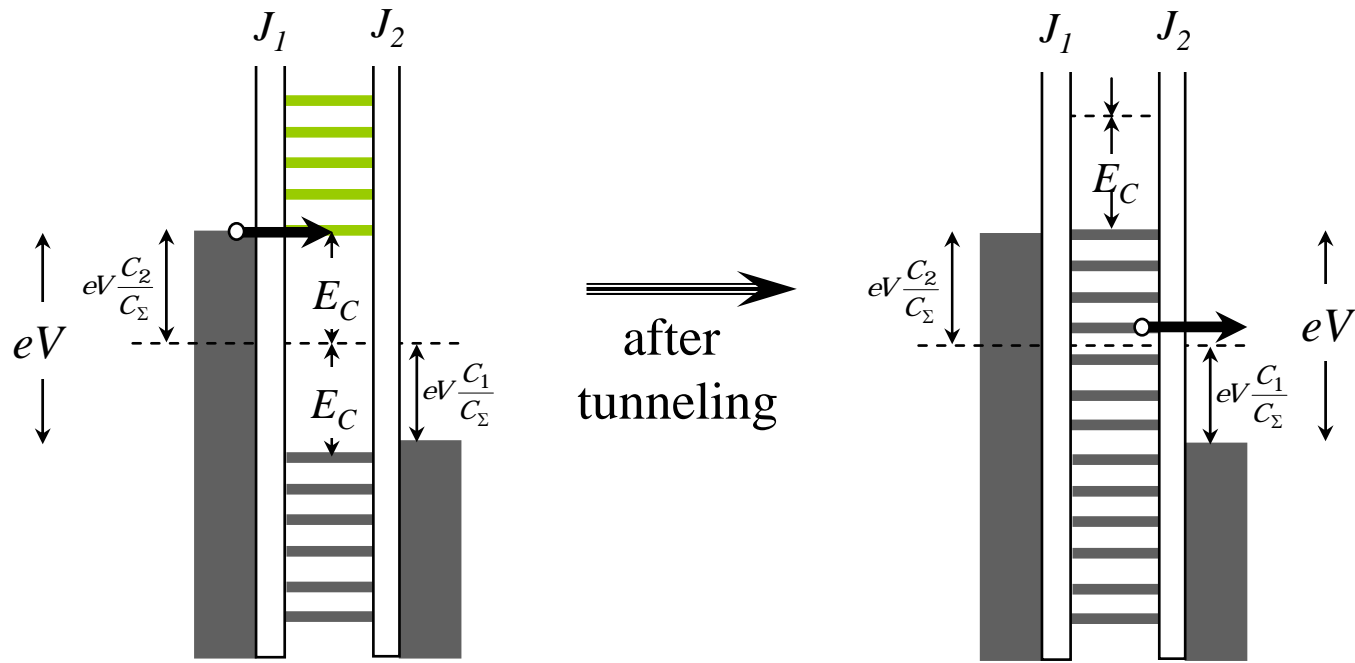
$$E_C \approx \frac{e^2}{C} \gg \frac{\hbar}{t_{\text{tunnel}}} \approx \frac{\hbar}{R_t C} \rightarrow R_t \gg \frac{\hbar}{e^2} \approx 26 \text{k}\Omega$$

For system in equilibrium: $t_{\text{relax}} \ll t_{\text{tunnel}}$

Nonequilibrium high electrons : hot electrons $t_{\text{relax}} \gg t_{\text{tunnel}}$







Nanomechanical oscillations in a single-C₆₀ transistor Nature 407, 57 (2000)

$$\frac{G}{G_\infty} = \frac{d/k_B T}{2 \sinh(d/k_B T)} \approx \frac{1}{2} \cosh^{-2} \left(\frac{d}{2.5 k_B T} \right)$$

For $h/t_{tunnel}, \delta \ll k_B T \ll E_C$

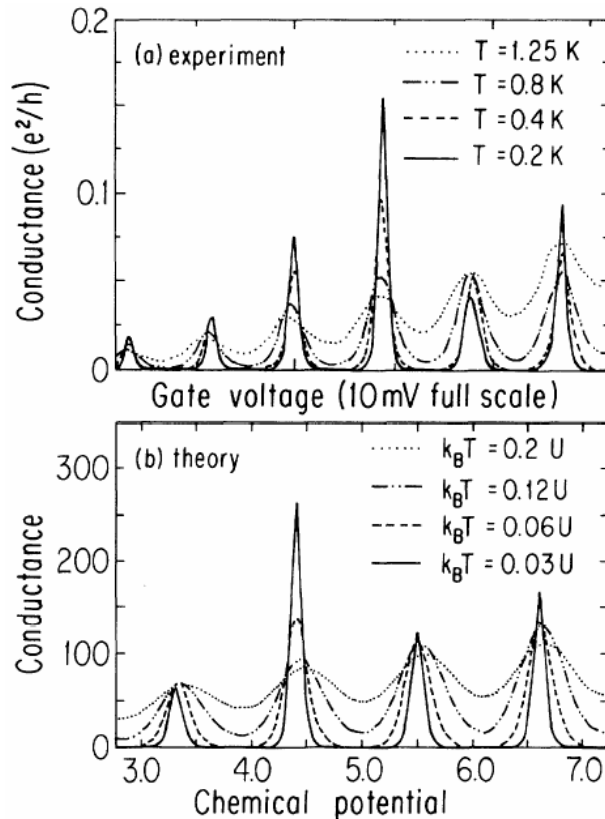


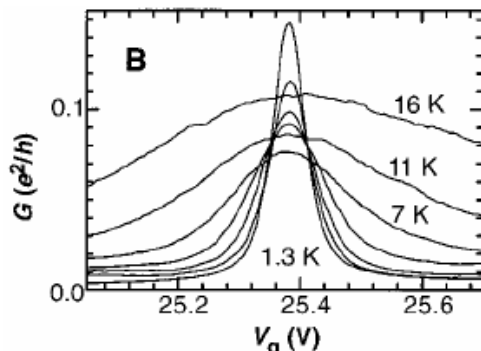
FIG. 2. (a) Experimental conductance of a narrow GaAs channel with two lithographically defined barriers plotted against gate voltage for four temperatures (Ref. 18). (b) Theoretical conductance, in units of $(\Gamma_1/U)(e^2/h)$, for ten levels, spaced by $\Delta\epsilon=0.1U$, vs chemical potential, in units of U , at four temperatures, calculated from (10). The elastic couplings of the levels increase geometrically, $\Gamma_n=1.5^n\Gamma_1$ (to simulate disorder Γ_4 is increased by an additional factor of 4). While for $k_B T \ll \Delta\epsilon$ only one bare level contributes to each conductance peak, for $k_B T=\Delta\epsilon$ many levels contribute, permitting the conductance to rise with temperature.

$$\frac{G}{G_\infty} = \frac{\delta}{4k_B T} \cosh^{-2} \left(\frac{d}{2k_B T} \right)$$

For $h/t_{tunnel} \ll k_B T \ll \delta, E_C$

$d = \text{distance from resonance}$

$$\frac{1}{G_\infty} = \frac{1}{G_{left}} + \frac{1}{G_{right}}$$



Science, 275, 1922 (97)

$$G_{BW} = \frac{2e^2}{h} \frac{(h/t_{tunnel})^2}{(h/t_{tunnel})^2 + d^2}$$

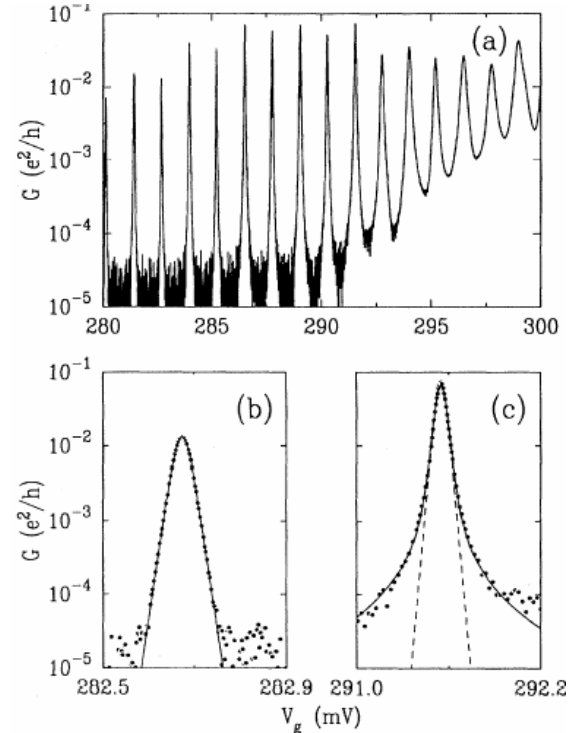


FIG. 3. (a) The low-bias conductance of the island vs V_g at $B=2.53$ T. [Note the alternation of peak amplitudes which arises from the spin splitting of levels (Ref. 17).] (b) A low V_g conductance peak from (a) shown fit to a thermally broadened resonance (solid line) in the limit that the intrinsic resonance width is much less than kT . (c) A conductance peak at higher V_g shown fit to a thermally broadened Lorentzian (solid line). The dashed line is the best fit using the same line shape as in (b).

Shell Filling and Spin Effects in a Few Electron Quantum Dot

S. Tarucha, PRL, 77, 3613 (96)

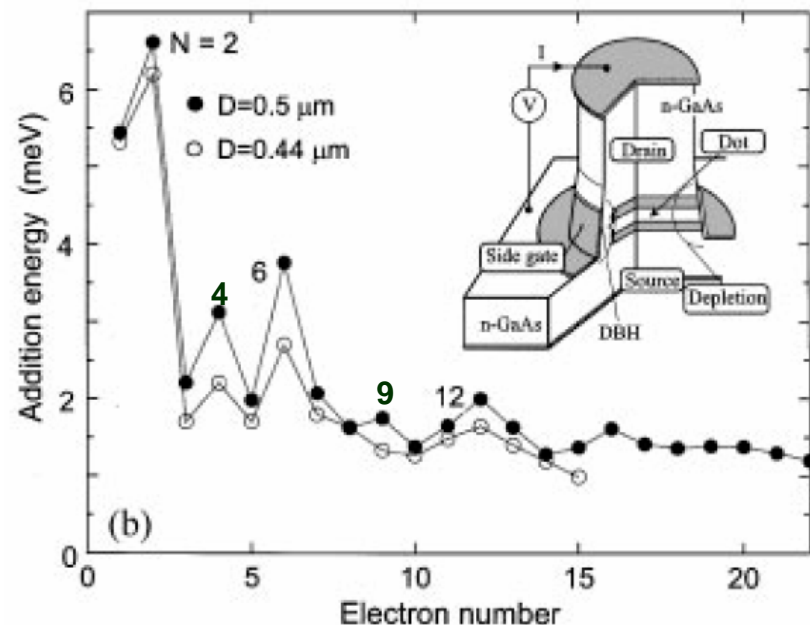
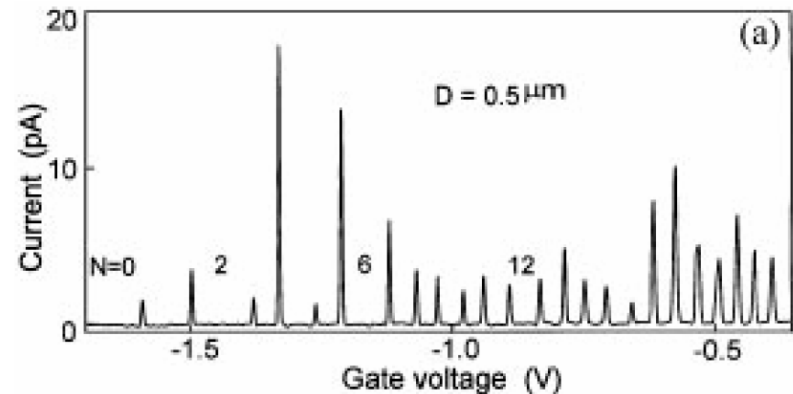
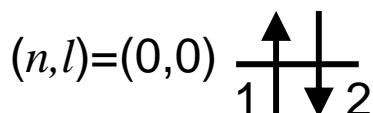
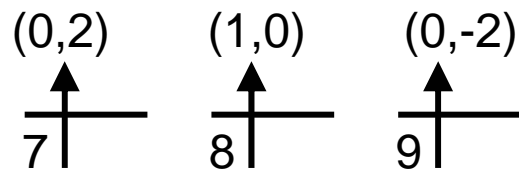
A harmonic confinement potential

$$V(r) = \frac{1}{2} m^* \omega_0^2 r^2$$

Eigenenergy: $E_{nl} = (2n + |l| + 1)\hbar\omega_0$

$$n = 0, 1, 2, \dots \quad l = 0, \pm 1, \pm 2, \dots$$

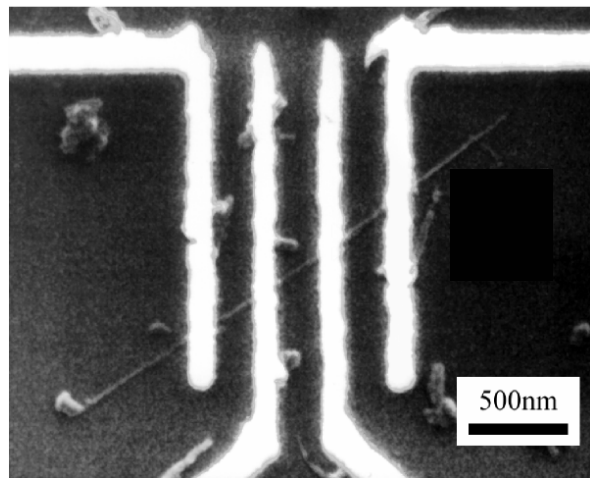
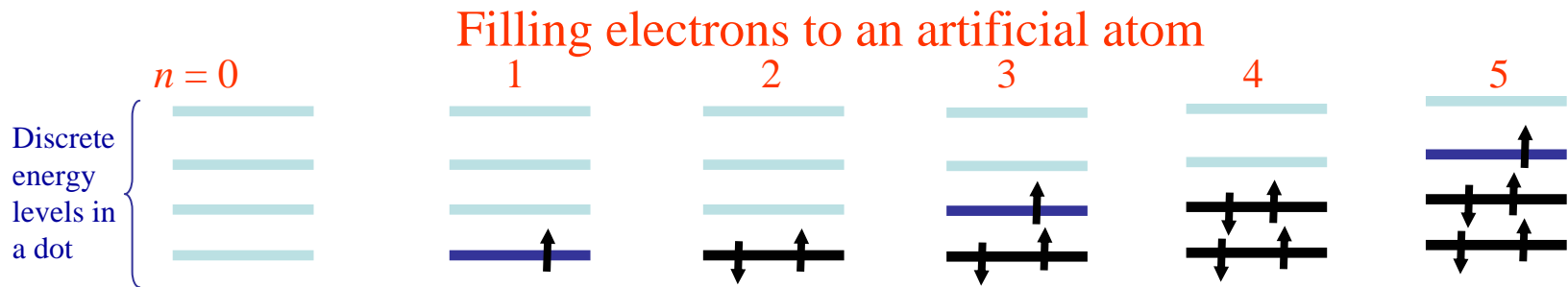
Hund's rule:



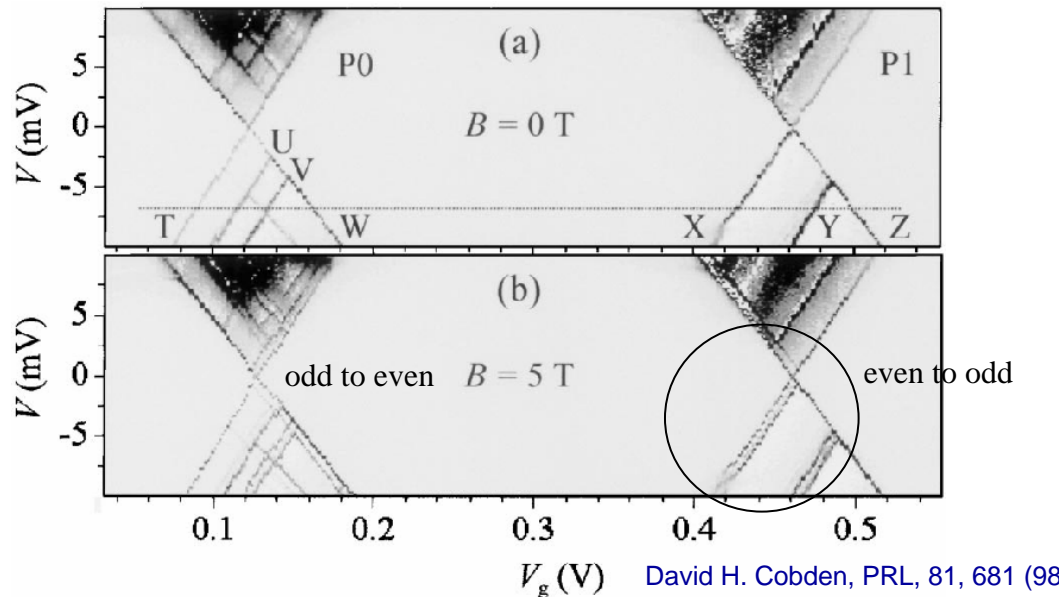
Transport through a quantum dot

Quantum dot is characterized by a finite energy level spacing ΔE

- each level contains two electrons of opposite spin
- the number of electrons in the dot is controllable, it is thus called **an artificial atom**
- entering of one electron causes island potential to increase by e/C or $e/C + \Delta E$ depending on the parity (even or odd) of the excess number of electrons



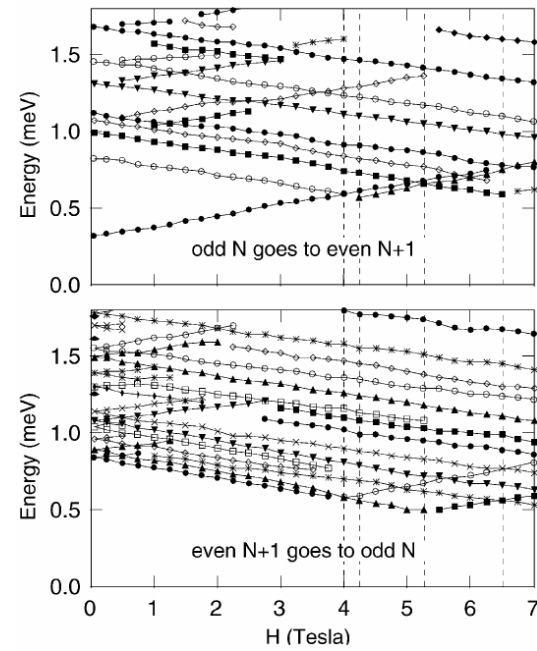
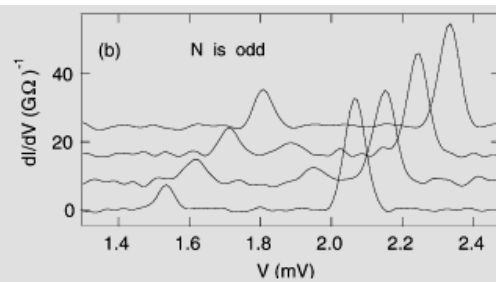
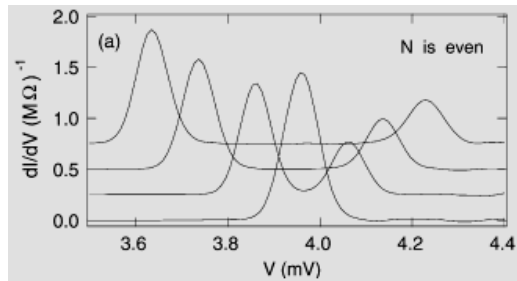
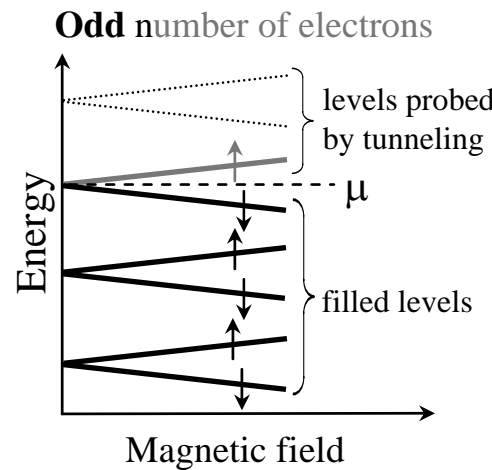
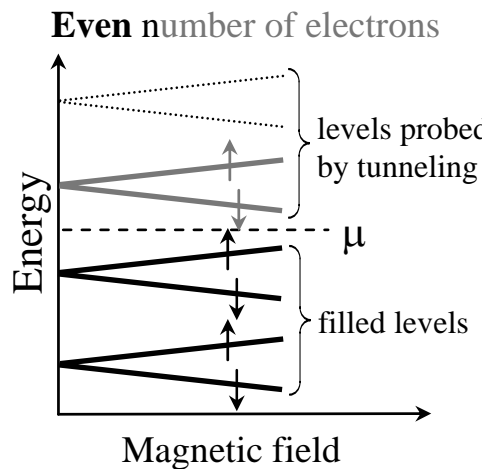
Adrian Bachtold, Nature, 397, 673 (99)

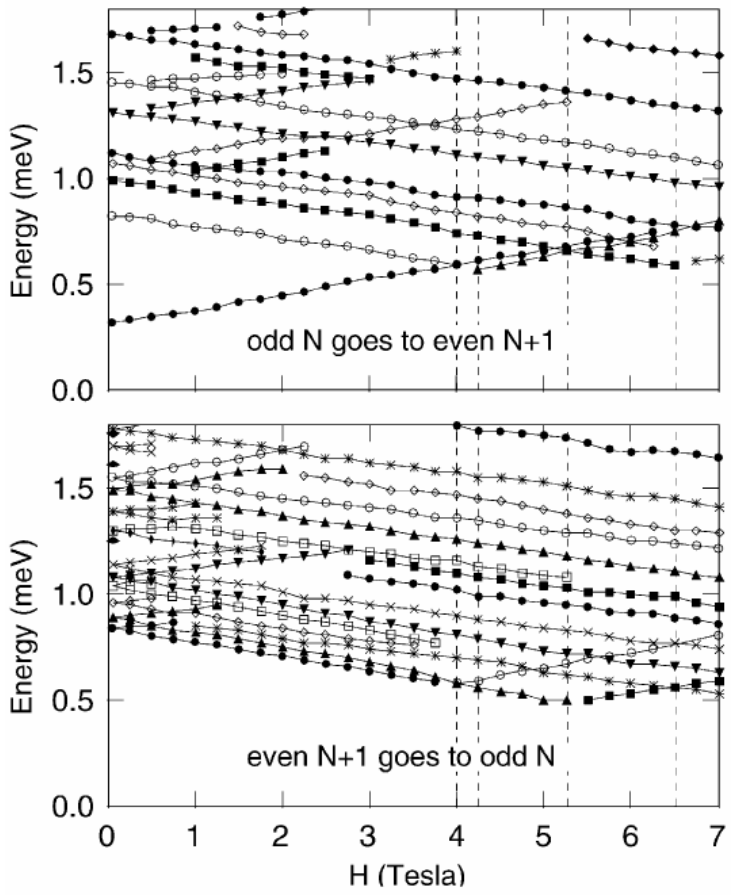


David H. Cobden, PRL, 81, 681 (98)

Electronic Spins in nano-particles: Zeeman Effect

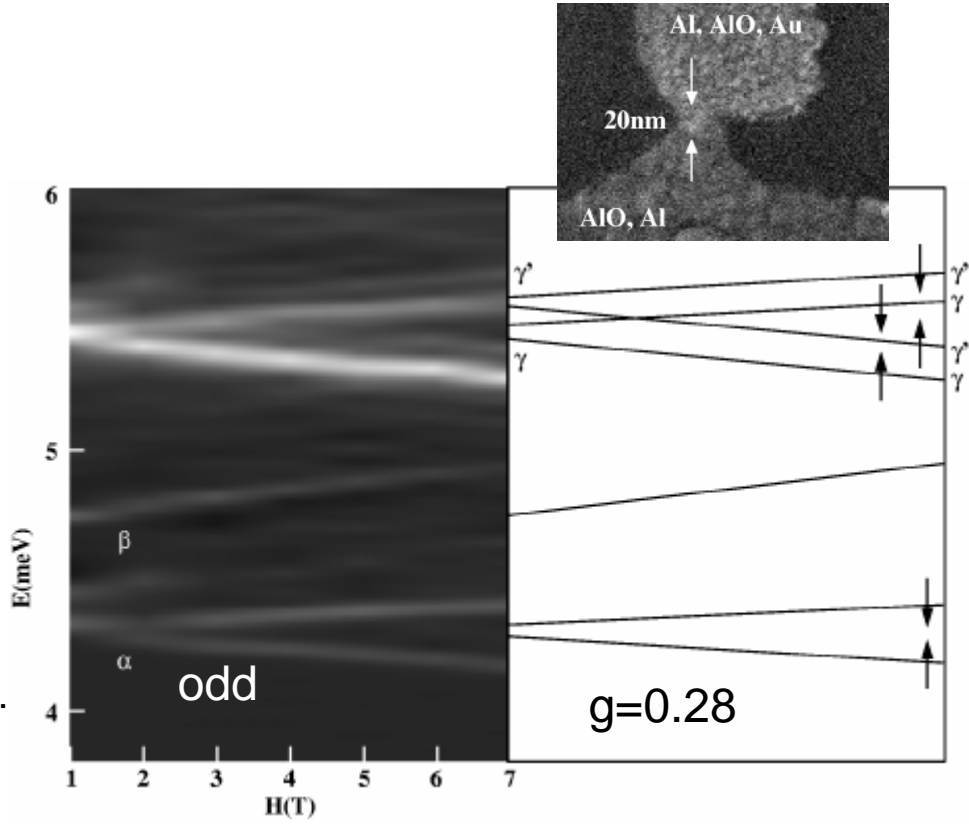
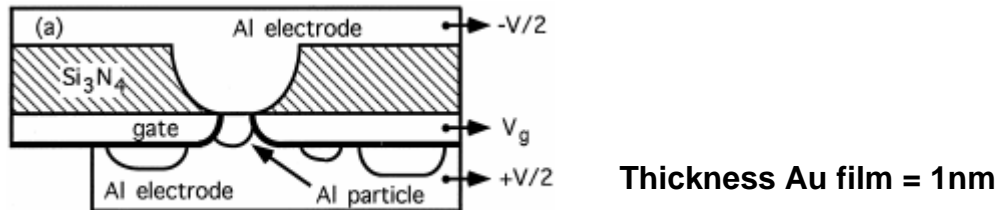
von Delft et al.
PRL, 77, 3189 (96)





D.C. Ralph, C.T. Black, M. Tinkham, Phys. Rev. Lett. 78 (1997) 4087.

Magnetic field dependence of the resolved electronic transitions for the device of Fig. 2 at (a) $V_g \approx 110$ mV and (b) $V_g \approx 180$ mV. The dashed lines show the average energy of the tunneling threshold at large H , corresponding to the (V_g -dependent) Coulomb barrier. $\Delta \approx 0.3$ meV.

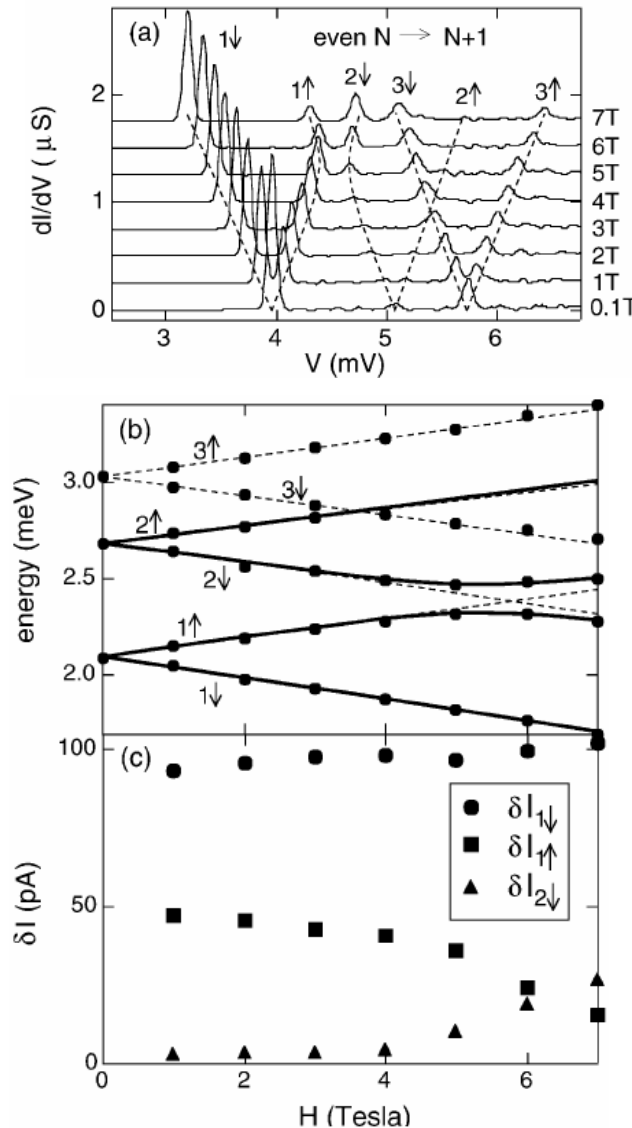


Magnetic field dependence of the energy spectrum in sample 1. Right schematic is a guide to the eye.

PRL, 83, 1644 (99)

Small g due to strong spin-orbit interaction

Effects of spin-orbit interactions on tunneling via discrete energy levels in metal nanoparticles
 PRB, 60, 6137 (99)



3nm Al-grain with $\sim 4\%$ Au impurities
 → Suppression of the g-factor

$$\delta E_j = g_j^{eff} \mu_B H \quad \mu_B = 57.8838 \mu eV/T \\ = \text{Bohr magneton}$$

Effective g factors
 1.84, 1.68 and 1.76

Particle size ~ 1-4 nm

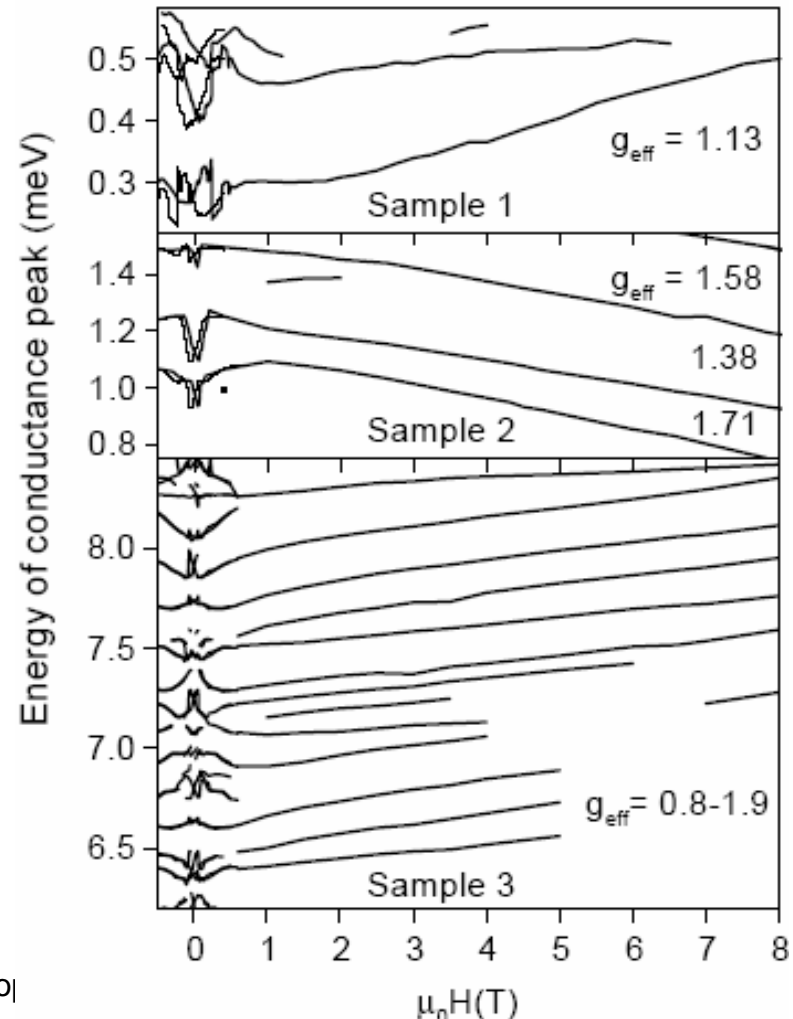
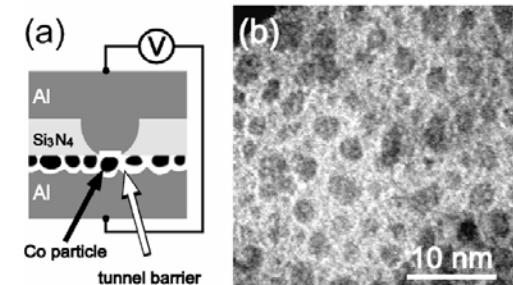
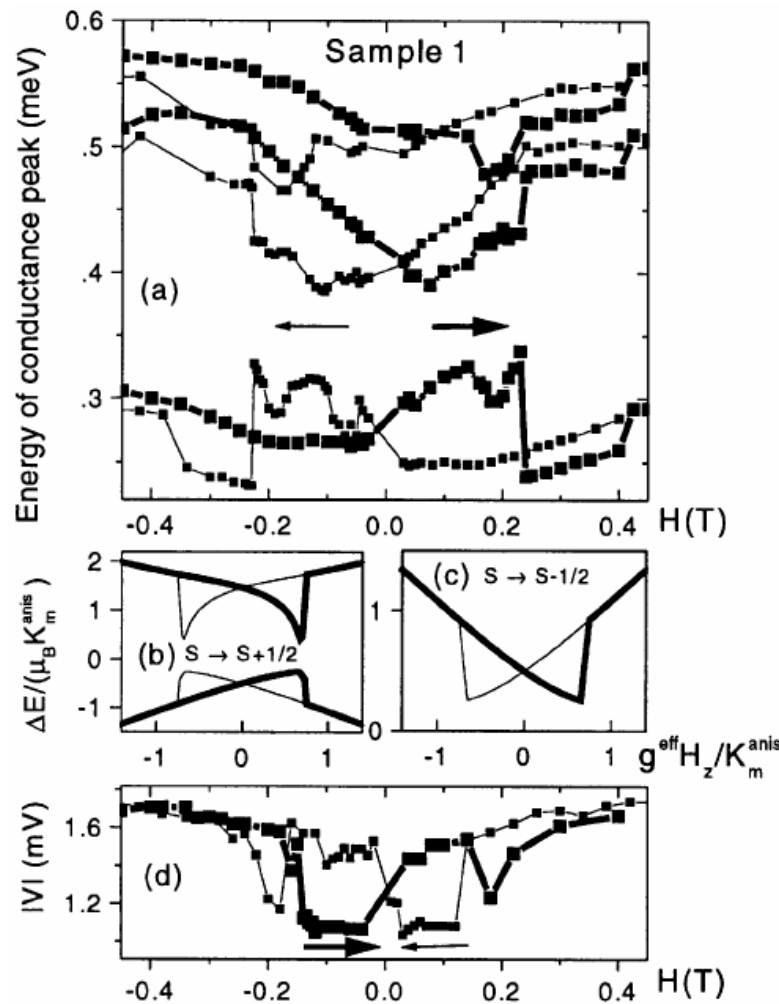
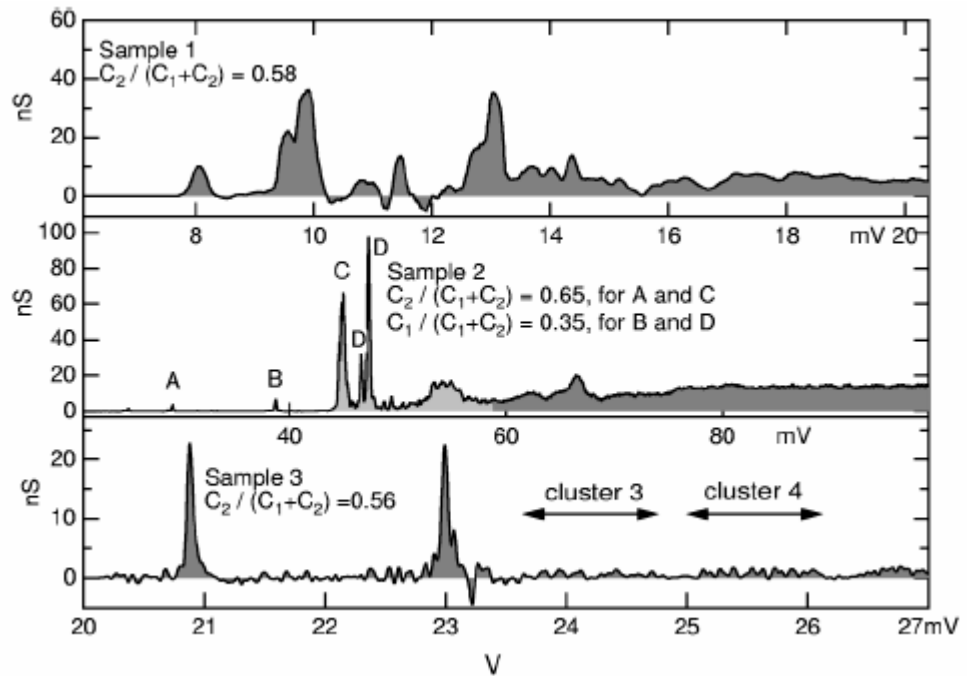


TABLE I. C_1 , C_2 , R_1 , and R_2 : junction capacitances and resistances determined from Coulomb staircase at 4.2 K. D : particle base diameter estimated from $C_1 + C_2$ assuming hemispherical shape. $\bar{\delta}$: estimated spacing between electron-in-a-box levels, based on particle volume. δ : measured level spacing. E_T : the Thouless energy of particles, estimated as $\hbar v_F / 3D'$, where D' is the particle base diameter corresponding to *measured* level spacing δ . g : determined from Zeeman splitting.

Sample	C_1 [aF]	C_2 [aF]	$R_1 + R_2$ [GΩ]	R_1/R_2	D [nm]	$\bar{\delta}$ [meV]	δ [meV]	E_T [meV]	Parity	g
1	4	5.5	0.15	7.9	9	0.65	1	37	odd	0.28
2	0.9	1.67	0.066	2	4.7	4.6	7	75	even	...
3	1.9	2.4	1.25	>25	6	2.1	1.2	40	odd	0.45

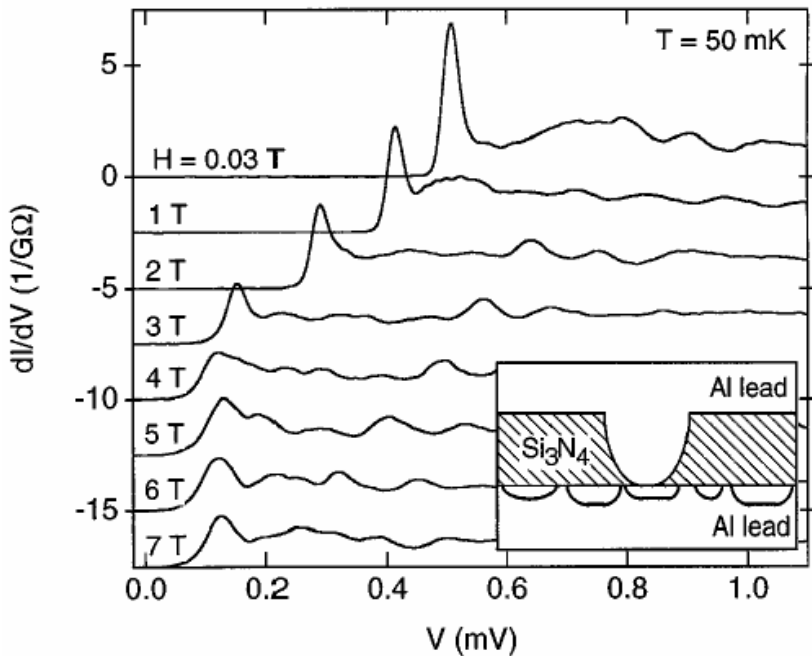
$$t_{travel} = 3D/v_F$$

$$E_T = \hbar/t_{travel} = \hbar v_F / 3D$$



Spectroscopy of the Superconducting Gap in Individual Nanometer-Scale Aluminum Particles

Particle size =2.5~4.5 nm



PRL, 76, 688 (96)

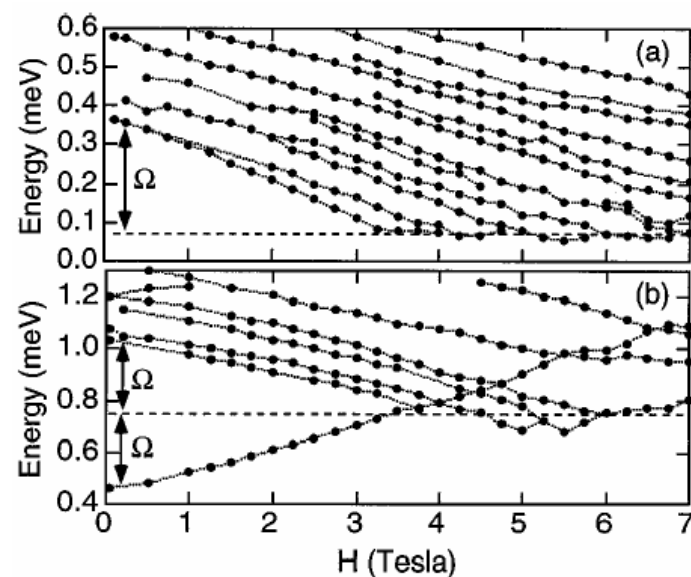


FIG. 2. Magnetic field dependence of resolvable transition energies at 50 mK for (a) sample 1, an even- n_0 particle and (b) sample 4, an odd- n_0 particle. Dotted lines are guides to the eye. Spacings in voltage have been converted to energy using the capacitance ratio $eC_1/(C_1 + C_2) = 0.73$ meV/mV for (a) and 0.66 meV/mV for (b).

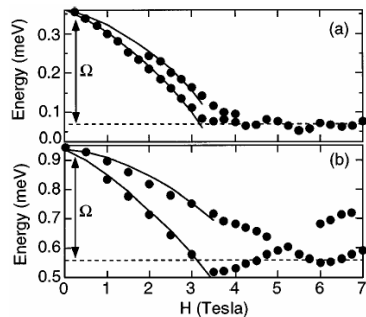


FIG. 3. Comparison of the predictions of orbital pair breaking plus Zeeman spin splitting (lines) to the measured field dependence of the lowest-energy tunneling transitions (dots) for (a) sample 1 and (b) sample 2.